



# **S5P/TROPOMI TOTAL BrO ALGORITHM TCBRO**

## **VALIDATION REPORT**



document number: S5P- BIRA-L2-TCBRO-VR

issue : 1.0.0  
date : 2022 01 09

## Document approval record

	digital signature
<b>prepared:</b>	Jeroen van Gent, François Hendrick
<b>Checked:</b>	
<b>approved PI:</b>	
<b>approved PM:</b>	

## Document change record

issue	date	item	comments
0.1.0	2020-07-24	All	Initial draft version
1.0.0	2022-01-09	All	First complete document version

## Contents

<b>Document approval record .....</b>	<b>2</b>
<b>Document change record .....</b>	<b>3</b>
<b>Contents .....</b>	<b>4</b>
<b>List of figures .....</b>	<b>5</b>
<b>List of tables .....</b>	<b>6</b>
<b>1 Introduction .....</b>	<b>7</b>
1.1 Identification .....	7
1.2 Purpose and objective .....	7
1.3 Document overview .....	7
1.4 Acknowledgements .....	7
<b>2 Applicable and reference documents .....</b>	<b>8</b>
2.1 Applicable documents.....	8
2.2 Standard documents .....	8
2.3 Reference documents.....	8
2.4 Electronic references .....	8
<b>3 Terms, definitions and abbreviated terms.....</b>	<b>9</b>
3.1 Terms and definitions .....	9
3.2 Acronyms and abbreviations.....	9
<b>4 Introduction .....</b>	<b>10</b>
4.1 The TCBRO L2 product .....	10
4.2 TCBRO configuration settings.....	10
4.3 The TCBRO dataset .....	12
4.4 Independent S5P BrO data .....	12
4.4.1 Satellite data.....	12
4.4.2 Ground-based data .....	13
<b>5 Slant column verification .....</b>	<b>14</b>
5.1 Comparison with GOME-2 data .....	14
5.2 Cross talk with HCHO .....	14
<b>6 The TCBRO vertical column density product .....</b>	<b>16</b>
6.1 Overall BrO distribution .....	16
6.2 Comparison with GOME-2 satellite data.....	17
6.2.1 Global BrO distribution in April 2019 .....	17
6.2.2 TROPOMI versus GOME-2 at 12 overpass sites. ....	18
6.3 TCBRO versus ground based data .....	20
<b>7 Conclusions .....</b>	<b>22</b>
<b>References .....</b>	<b>26</b>

## List of figures

<b>Figure 1: BrO, HCHO, and O<sub>3</sub> absorption cross-section in the UV convolved at the spectral resolution of S5-P. The data sets are normalized to arbitrary units for visibility. ....</b>	<b>10</b>
<b>Figure 2: Dependency of the retrieved TCBRO slant column on the boundaries of the wavelength fitting window. The lower boundary was varied between 328 and 335.5 nm. The upper boundary was varied between 358 and 359 nm. The values are averaged SCD over an Arctic geographic region.....</b>	<b>11</b>
<b>Figure 3: Slant column data for 24 March 2019, for the latitude band [-30°, 30°]......</b>	<b>11</b>
<b>Figure 4: Comparison of slant column densities for TROPOMI, GOME-2B, and GOME-2C for 24 March 2019. The black polygons indicate the Pacific zone between -25 and + 25 degrees latitude used in Section 5.2. ....</b>	<b>14</b>
<b>Figure 5: Pacific uncorrected BrO (left) and HCHO (right) slant column density as function of swath scan position for one orbit of 24 March 2019. a: TROPOMI; b: GOME-2B; c: GOME-2C.....</b>	<b>15</b>
<b>Figure 6: Monthly average TCBRO BrO vertical column density (VCD) for the entire northern hemisphere, for selected months in 2019. ....</b>	<b>16</b>
<b>Figure 7: Geophysical distribution of the BrO vertical column density, averaged over April 2019 .....</b>	<b>17</b>
<b>Figure 8: The Ground measurements stations for which satellite overpass data is compared in this document. ....</b>	<b>18</b>
<b>Figure 9: Comparison of TCBRO, GOME-2B, and GOME-2C BrO vertical column data over 12 ground stations. ....</b>	<b>20</b>
<b>Figure 10: Daily BrO vertical column data as measured from Harestua (red) and with TROPOMI (blue). The two datasets agree well for the period March-October 2019. ....</b>	<b>21</b>
<b>Figure 11: S5P/TROPOMI monthly average BrO vertical column density (VCD) for the full year 2019. Left column: North Pole region; middle column: global distribution (Mercator); right column: South pole region.....</b>	<b>25</b>

## List of tables

<b>Table 1: TCBRO slant column fitting configuration settings. ....</b>	<b>12</b>
<b>Table 2: Offset of the satellite BrO VCD data sets with respect to the Harestua zenith-sky measurements.....</b>	<b>20</b>

# **1 Introduction**

## **1.1 Identification**

This document describes the verification and validation of one year of TCBRO L2 data by means of comparisons with independent datasets. The TCBRO version described in this document is version 1.1.1.

## **1.2 Purpose and objective**

The purpose of the document is to assess the quality of TCBRO derived BrO columns from S5P measurements. The objective is to give insight in the current quality of the results and remaining work to be done.

## **1.3 Document overview**

Chapter 2 lists applicable and reference documents. Chapter 3 gives relevant terms and definitions. The actual data comparison is presented in chapter 4.

## **1.4 Acknowledgements**

The authors would like to thank the following people for their kind assistance in the presented work: Sora Seo (now at DLR) and Andreas Richter from IUP-UB in Bremen.

## **2 Applicable and reference documents**

### **2.1 Applicable documents**

There are no applicable documents

### **2.2 Standard documents**

There are no standard documents

### **2.3 Reference documents**

- [RD01] Terms, and symbols in the TROPOMI Algorithm Team; source: KNMI; ref: SN-TROPOMI-KNMI-L2-049-MA; issue: 1.0.0; date: 2015-07-16
- [RD02] Quarterly Validation Report of the Copernicus Sentinel-5 Precursor Operational Data Products; ref: S5P-MPC-IASB-ROCVR; issue: 6.0.1; date: 2020-03-30.
- [RD03] S5p L2 Algorithm Theoretical Basis Document– TCBRO; source: BIRA; reference: S5P-L2-BIRA-ATBD-TCBRO; version: 01.00.00; date: 2022-01-12
- [RD15] Sentinel-5 Precursor Level 2 UPAS Processor Input / Output Definition Document; source: DLR; ref: S5P-L2-DLR-IODD-3002; issue: 3.5.0; date: 2019-08-09.

### **2.4 Electronic references**

- [URL01] <http://uv-vis.aeronomie.be/software/QDOAS/>
- [URL02] [http://uv-vis.aeronomie.be/software/QDOAS/QDOAS\\_manual.pdf](http://uv-vis.aeronomie.be/software/QDOAS/QDOAS_manual.pdf)
- [URL03] <https://atmospherictoolbox.org/>
- [URL04] <http://mpc-vdaf.tropomi.eu/>

### 3 Terms, definitions and abbreviated terms

Terms, definitions and abbreviated terms that are used in the development program for the TROPOMI L2 data processors are described in [RD02]. Terms, definitions and abbreviated terms that are specific for this document can be found below.

#### 3.1 Terms and definitions

No additional terms at this point

#### 3.2 Acronyms and abbreviations

AC-SAF	Atmospheric Composition Science application Facility
AMF	Air Mass Factor
BrO	Bromine Monoxide
DOAS	Differential Optical Absorption Spectroscopy
GOME-2	Global Ozone Monitoring Experiment–2
L2	Level-2
MetOp	Meteorological Operational Satellite
O <sub>3</sub>	Ozone
SCD	Slant Column Density
SZA	Solar Zenith Angle
TROPOMI	Tropospheric Monitoring Instrument
VCD	Vertical Column Density
VZA	Viewing Zenith Angle

## 4 Introduction

### 4.1 The TCBRO L2 product

The TCBRO algorithm for the derivation of L2 total vertical BrO column data was developed in the framework of the ESA-funded S5P-PAL project, coordinated by S&T. The algorithm follows a DOAS scheme: a slant column fitting procedure is followed by an offset correction step and finally the corrected slant columns are converted into vertical columns by mean of a geometric air mass factor (AMF). The choice of a geometric AMF was historically found to be accurate for total BrO column derivation, due to the significant BrO stratospheric content and the often high surface reflectance in areas with enhanced tropospheric BrO. This may be further refined in future update of the algorithm.

The algorithm uses daily averaged radiance data over a clean, Pacific region as reference data. The reference data is calculated by a dedicated auxiliary algorithm, called BGBRO, which is supposed to be run separately in order to make the reference data available before TCBRO is executed.

A full description of the algorithm details of both TCBRO and BGBRO is given in [RD03]. The TCBRO dataset subject to validation and used in this document is the full year 2019, obtained with TCBRO processor version 1.1.1.

Validation of other, operational TROPOMI L2 products is performed quarterly by the Mission Performance Center MPC. For recent validation results, see [RD02] or [URL04]

### 4.2 TCBRO configuration settings

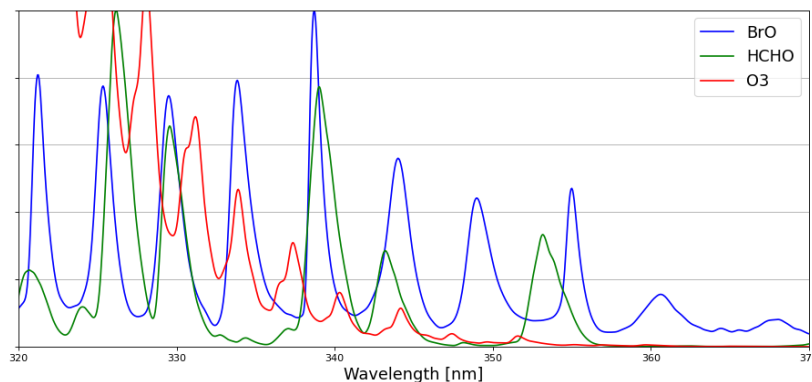


**Figure 1:** BrO, HCHO, and O<sub>3</sub> absorption cross-section in the UV convolved at the spectral resolution of S5-P. The data sets are normalized to arbitrary units for visibility.

Bromine Monoxide has its strongest absorption bands in the 310-365 nm wavelength range (Figure 1). For the short wavelengths in this range, the BrO signal however suffers from a strong increase in Rayleigh scattering and ozone absorption. In practice, this leads to a very small BrO signal in the satellite spectra compared to ozone absorption, especially for tropospheric BrO. Consequently, BrO is traditionally retrieved (for GOME, SCIAMACHY, GOME-2, OMI, TROPOMI) using fitting windows in the 319-360 nm range. The derivation of the optimal BrO fitting window is not straightforward and small shifts of one of the fitting window boundaries may result in significant changes in the derived slant columns density (SCD). The interference of ozone or formaldehyde absorption are in part behind this, but the window selection depends also on the observed scene type or on instrumental characteristics and it may even be necessary to adapt the fitting window with time (e.g. Bougoudis et al., 2020).

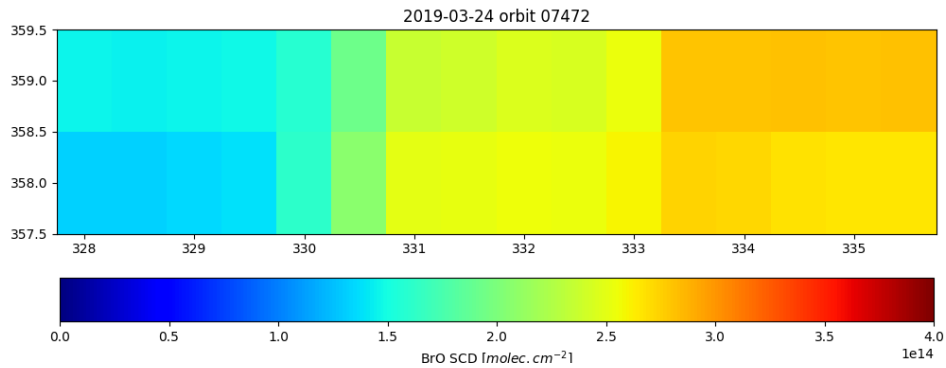


**Figure 2:** Dependency of the retrieved TCBRO slant column on the boundaries of the wavelength fitting window. The lower boundary was varied between 328 and 335.5 nm. The upper boundary was varied between 358 and 359 nm. The values are averaged SCD over an Arctic geographic region.

For S5P/TROPOMI, an extensive fitting window sensitivity study was performed in Seo et al. (2019). Studying different scene types, this study determined a best overall fitting window of 334.6-358 nm.

For the S5P TCBRO algorithm, this window was initially adopted as the baseline. A direct algorithm comparison between TCBRO and the algorithm from Seo et al. (2019) was performed by means of a kindly provided set of slant column data for one day in March 2019 (Sora Seo, private communication). Although results came close, remaining differences of 10-15% were observed for elevated BrO concentrations, thought to be the results of a different treatment of the Ring effect in the respective fits.

Similar positive offsets were also encountered when performing first TCBRO VCD comparisons with Harestua ground-based measurements.

A logical alternative would be to use the wider fitting window of 328.5-259 nm, used for BrO pre-fitting in the TROPOMI formaldehyde algorithm, developed at BIRA-IASB. One of the advantages would be the inclusion of more spectral data points, which would reduce the slant column RMSE over regions with low BrO content. In testing this window, this was indeed observed (Figure 3). See also Seo et al. (2019).

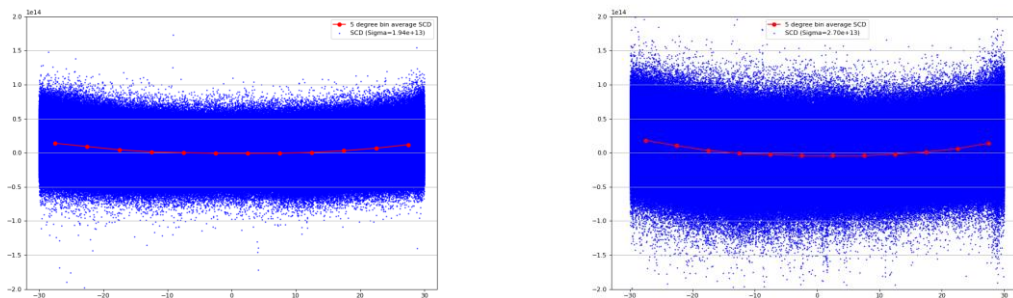


**Figure 3:** Slant column data for 24 March 2019, for the latitude band  $[-30^\circ, 30^\circ]$ .

In testing the window from the HCHO product, however, we found lower BrO columns in comparison to the Harestua data and we therefore performed a small sensitivity study on the start wavelength of the fitting window. Based on the results depicted in Figure 2, it was finally decided to adopt a fitting window of 332-359 nm, which is identical to the window used in GOME-2 BrO retrievals (Theys et al., 2011). Upon inspection of Figure 1, this window has the advantage that it included one additional BrO absorption peak in comparison to the 334.6-358 window, and at the same time avoids the formaldehyde absorption feature around 330 nm that is included in the 328.5-359 nm window.

Although the window selection is to some degree arbitrary, analysis of more scenes over longer periods of time is expected to provide further insight in the details of the retrieval results and the retrieval settings may be updated in a future algorithm version. The current TCBRO configuration settings are listed in Table 1.

### 4.3 The TCBRO dataset

The dataset that is subject to validation in this report comprises one year (2019) of total BrO VCD data. This data was derived with TCBRO processor version 1.1.1 on the S5P-PAL processing environment.

### 4.4 Independent S5P BrO data

For the validation of the TCBRO data, datasets were selected that are known to be accurate and have been validated themselves against independent measurements. These datasets are described below.

<b>Fitting window</b>	332-359 nm
<b>O<sub>3</sub> 223K &amp; 243K</b>	Serdyuchenko et al., 2014
<b>BrO 223K</b>	Fleischman, 2003
<b>NO<sub>2</sub> 220K</b>	Vandaele et al., 1998
<b>HCHO 298K</b>	Meller & Moortgat, 2000
<b>OCIO 213K</b>	Bogumil et al. 2003
<b>O<sub>4</sub> 293 K</b>	Thalman & Volkamer, 2013
<b>Ring</b>	From SAO2010 solar spectrum, ratio raman/solar
<b>Polynomial</b>	5 coeff. (4 <sup>th</sup> order)
<b>Offset correction</b>	Linear
<b>Equatorial offset correction</b>	None

Table 1: TCBRO slant column fitting configuration settings.

#### 4.4.1 Satellite data

##### 4.4.1.1 GDP 4.8 MetOp-B/GOME-2

BrO L2 VCD data from the MetOp-B/GOME-2 instrument (GOME-2B) is operationally retrieved at DLR and readily available at our institute. For the validation of TCBRO, the offline version of the the GOME-2B BrO product is used. The GOME-2B version GDP 4.8 data were validated in the framework of the EUMETSAT AC-SAF and found to be within the target accuracy (30%) and even within the optimal accuracy (15%) if the tropospheric content is considered in the comparison with ground-based data (Theys et al., 2015).

#### 4.4.1.2 GDP 4.9 MetOp-C/GOME-2

Although GDP4.9 MetOP-C/GOME-2 (GOME-2C) data is now operationally made available at DLR, this was not yet the case 2019. After the MetOp-C launch on 18 November 2018, the year 2019 was largely covered by commissioning activities. Six months (February-July 2019) of early GOME-2C data was made available to BIRA-IASB in the frame of AC-SAF validation activities. The validation is described in Merlaud et al. (2020).

### 4.4.2 Ground-based data

#### 4.4.2.1 Harestua

Ground-based total BrO columns at Harestua, Norway (Hendrick et al., 2007, 2008, 2009) are available from operational zenith-sky measurements. BIRA-IASB is operating ground-based DOAS systems at several ground-stations: Beijing, Harestua, Jungfraujoch, and Observatoire de Haute-Provence.

## 5 Slant column verification

### 5.1 Comparison with GOME-2 data

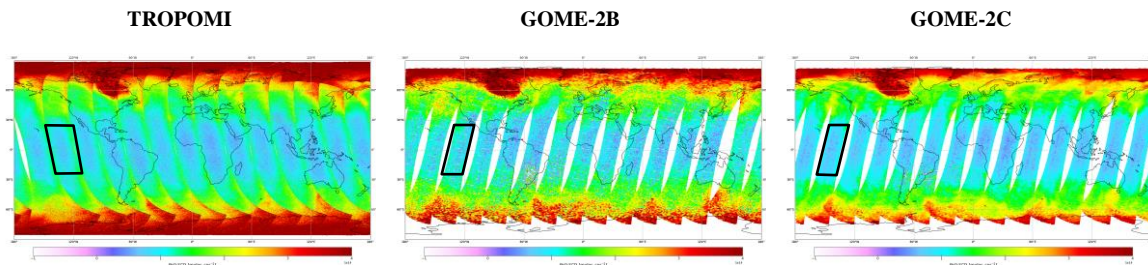


**Figure 4:** Comparison of slant column densities for TROPOMI, GOME-2B, and GOME-2C for 24 March 2019. The black polygons indicate the Pacific zone between  $-25$  and  $+25$  degrees latitude used in Section 5.2.

Figure 4 shows one day of (offset-corrected) SCD results for TCBRO/TROPOMI BrO, along the equivalent data from GOME-2B and -C. In this qualitative comparison, a very good agreement of the TCBRO results with the GOME-2 sensors is observed. GOME-2C shows some increased SCD values at the eastern and western edges of the orbit swaths, something which can be expected from the  $1/\cos(\theta)$  dependency on the viewing zenith angle in the AMF (larger slant columns at the swath edges). This is, however, not as clearly seen in the GOME-2B results, but this may be due to the noisier signal. The effect is most pronounced in the TROPOMI data; with its wider swath this is not surprising. The black trapezium shaped polygons in the figure will be explained in section 5.2.

### 5.2 Cross talk with HCHO

One aspect that the retrieval of BrO and formaldehyde have in common is that one species affects the retrieval of the other due to overlapping absorption cross-section maxima in the UV spectral range and this phenomenon is one of the major aspects in finding a suitable fitting window. Still, some cross-talk between the species may remain and this is investigated in this section by looking at the viewing angle dependence of non-background corrected BrO and HCHO slant columns for the SCD's from TCBRO, GOME-2B, and GOME-2C. In case of cross-talk, an increase of derived SCD towards the edge of the swath for one species, would be mirrored by a negative trend for the other species.

In order to study this, we look at one orbit of 24 March 2019 over the Pacific, for each instrument in the latitude interval  $[-25^\circ, 25^\circ]$  (black polygons in Figure 4). Here, there should be a low but homogeneous HCHO background concentration from methane oxidation.

Figure 5 shows the VZA angle dependency of the BrO and HCHO SCD's by indicating the SCD values as function of across-track pixel index. The mirror effect introduced above is clearly visible for GOME-2C, but is less pronounced for GOME-2B. The TROPOMI measurements do not seem to indicate any indication of BrO-HCHO cross talk, likely due to better instrument characteristics.

The differences between the two GOME-2 instruments are described in more detail in Merlaud et al. (2020).

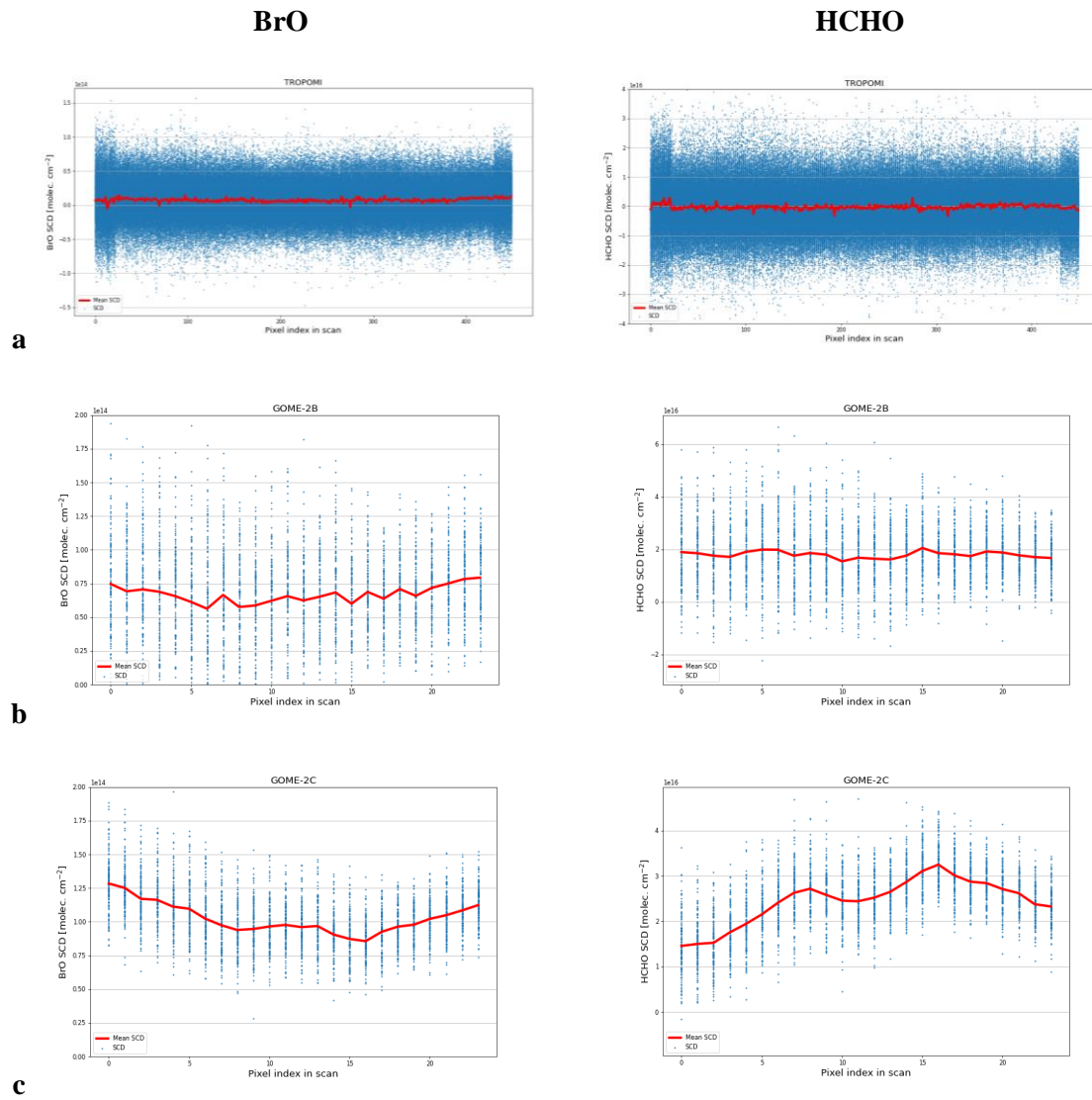


**Figure 5:** Pacific uncorrected BrO (left) and HCHO (right) slant column density as function of swath scan position for one orbit of 24 March 2019. **a:** TROPOMI; **b:** GOME-2B; **c:** GOME-2C.

## 6 The TCBRO vertical column density product

In the sections below, we evaluate the TCBRO BrO vertical column density (VCD) product through comparison with data from other satellite sensors and from ground based measurements.

### 6.1 Overall BrO distribution

Monthly averaged TCBRO VCD columns for the Northern hemisphere are shown in Figure 6. The overall BrO geophysical distribution patterns agree well with those known from literature, with highest total columns in spring and lowest quantities in late summer. Large scale patterns show enhanced BrO as far south as Northern Africa, consistent with stratospheric BrO distributions (e.g. Theys et al, 2007; 2009). More localized patterns include the spring bromine explosion event in the image of March and enhanced BrO over the Rann of Kutch salt desert straddling the India-Pakistan border in the data for March and May.

Images of monthly averaged TCBRO VCD data for the full year 2019 can be consulted in Appendix A.

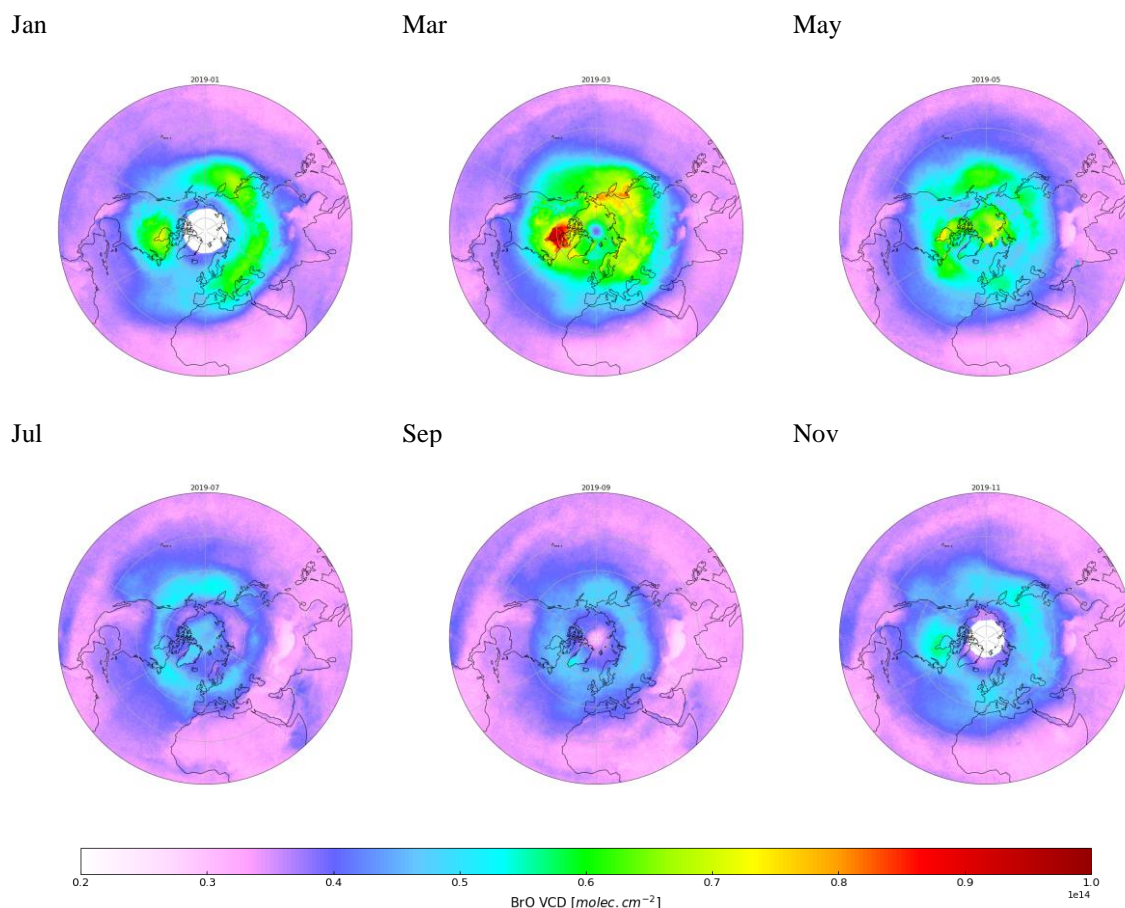


**Figure 6:** Monthly average TCBRO BrO vertical column density (VCD) for the entire northern hemisphere, for selected months in 2019.

## 6.2 Comparison with GOME-2 satellite data.

### 6.2.1 Global BrO distribution in April 2019

Here, the TCBRO VCD distribution is compared to those derived from the GOME-2 sensors on the MetOp-B and MetOp-C platforms. A comparison of the global geophysical distribution is depicted in Figure 7. The patterns derived from the TROPOMI measurements agree very well with those from GOME-2B and GOME-2C and show an overall smoother signal. TROPOMI is also more sensitive to locally enhanced BrO, like over the Rann of Kutch salt marshes in northwest India and is less sensitive to the South Atlantic anomaly. The latter is particularly visible in the GOME-2B signal, a sign of instrument degradation. On closer inspection, the elevated BrO patterns of TROPOMI also show differences when compared to the GOME-2 instruments. Part of this may be due to diurnal variation of the BrO concentration, as TROPOMI has an early afternoon local overpass time of 13h30, whereas the GOME-2 instruments observe at 9h30. Still, other effects may play a role and a quantitative comparison is performed in the next section.

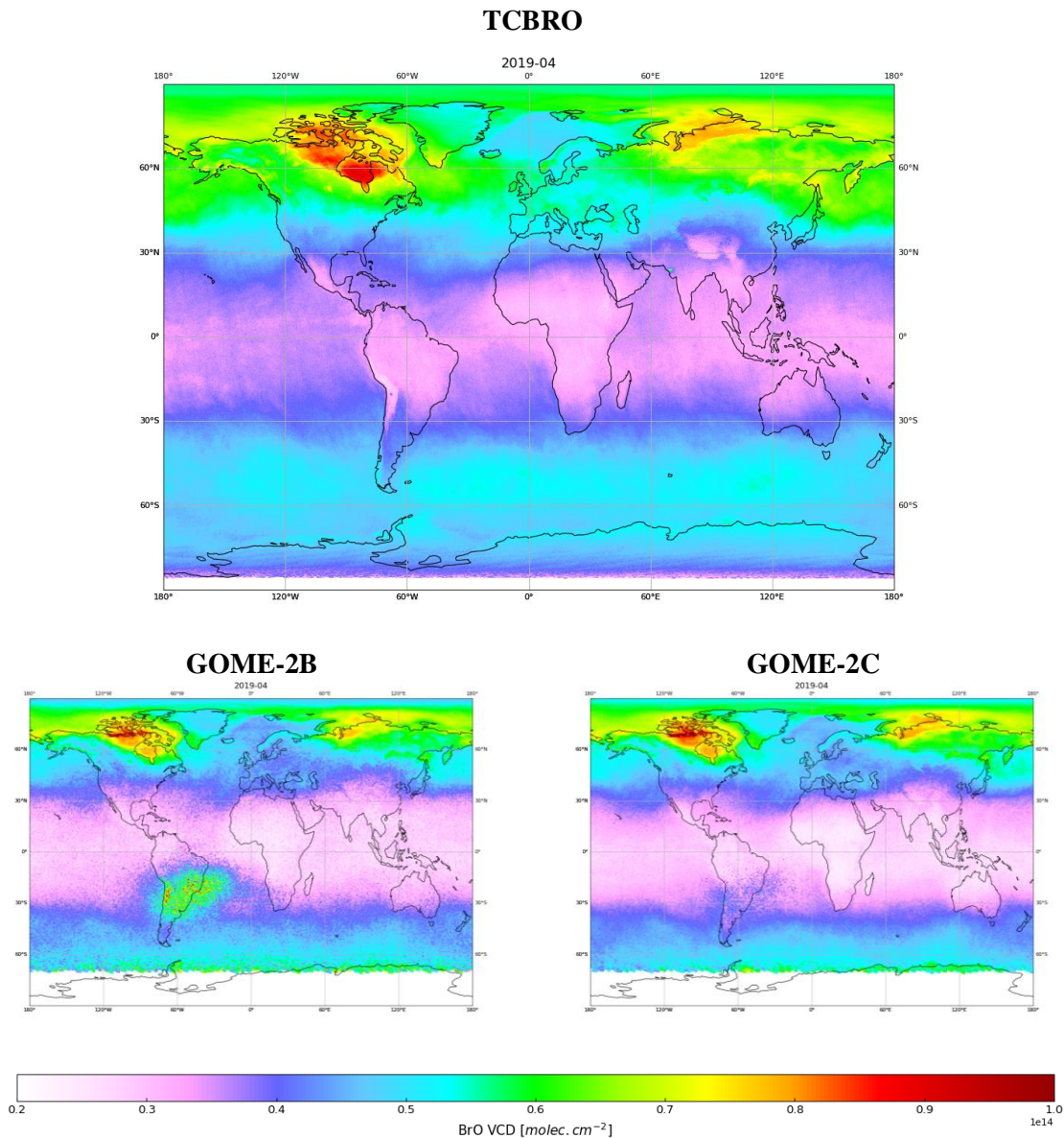


**Figure 7:** Geophysical distribution of the BrO vertical column density, averaged over April 2019

## 6.2.2 TROPOMI versus GOME-2 at 12 overpass sites.

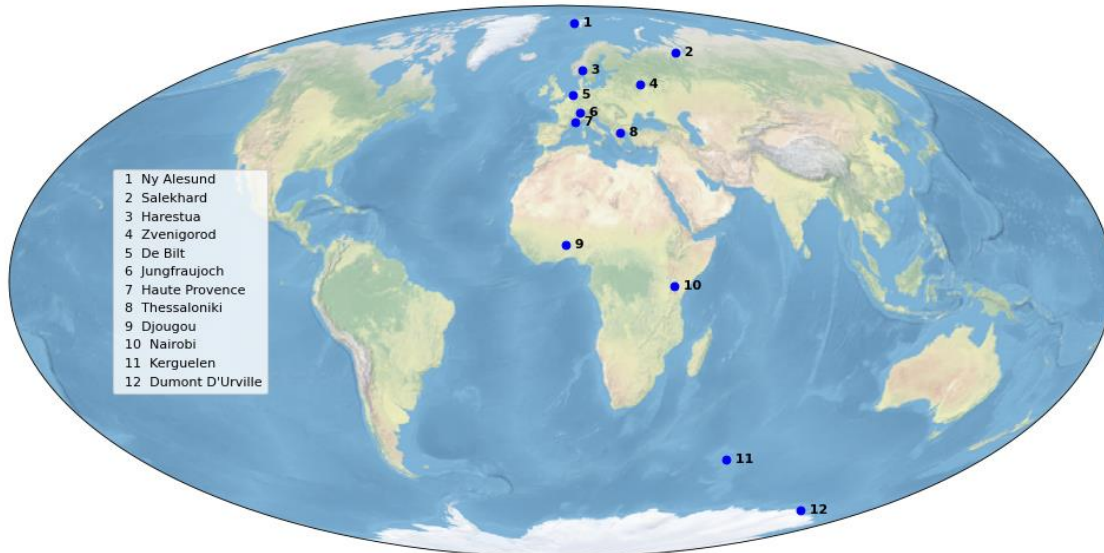


**Figure 8:** The Ground measurements stations for which satellite overpass data is compared in this document.

In order to quantify the agreement between TCBRO and GOME-2 BrO VCD, monthly averaged VCD values have been derived for 12 discrete locations covering almost the full geographical latitude range. These locations correspond to well-known stations for ground based atmospheric measurements and for which GOME-2 trace gas overpass data is routinely determined. The stations are visualized in Figure 8.

Figure 9 compares the TCBRO TROPOMI results with GOME-2 VCD values at the 12 stations. The two GOME-2 instruments closely agree with each other and an analysis of the mutual agreement of GOME-2B and GOME-2C BrO values was performed in Merlaud et al. (2020). The TCBRO monthly average VCD values largely follow the seasonal pattern of the GOME-2 VCD's. However, the TCBRO values are often higher than those from GOME-2, in particular in July and August for stations at northern mid latitudes. A firm explanation of the positive offset of the TCBRO VCD's cannot be given at this moment, but the phenomenon is likely due to a mixture of effects. AMF effects may play a role, but the wider swath width of TROPOMI indicates larger AMF values, from which smaller VCD's would be expected. Albedo effects may explain why the agreement worst in local summer months for stations at large latitudes, as the geometric approximation of the TCBRO AMF is the less accurate. On the other hand, Merlaud et al. (2020) showed that the GOME-2B ( $-15 \pm 11\%$ ) and GOME-2C ( $-12 \pm 10\%$ ) VCD's compare low to Harestua zenith-sky measurements, possibly explaining part of the differences with the TCBRO columns. For a better understanding, a comparison of the TCBRO columns with ground measurements is required, which is the subject of section 6.3.

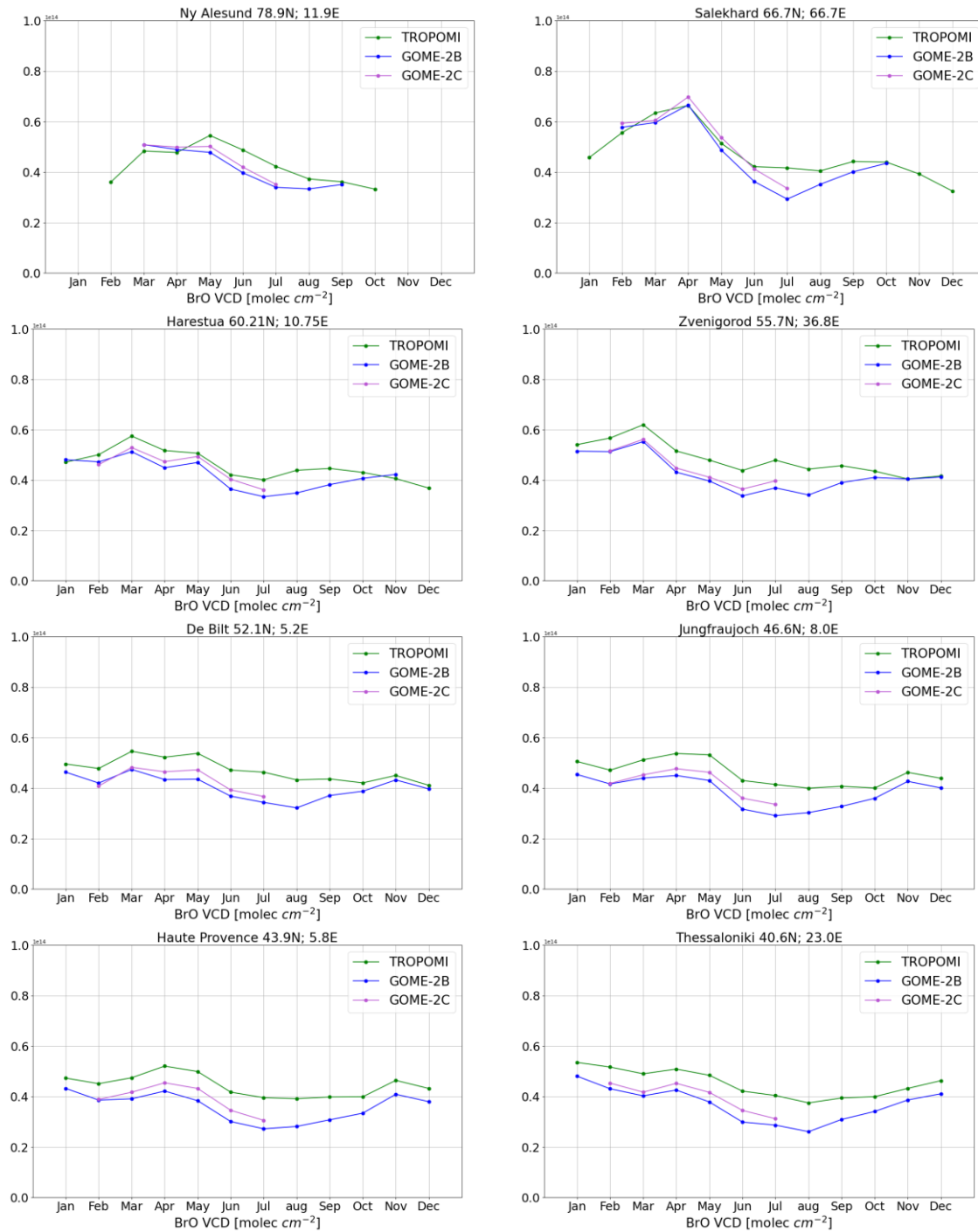
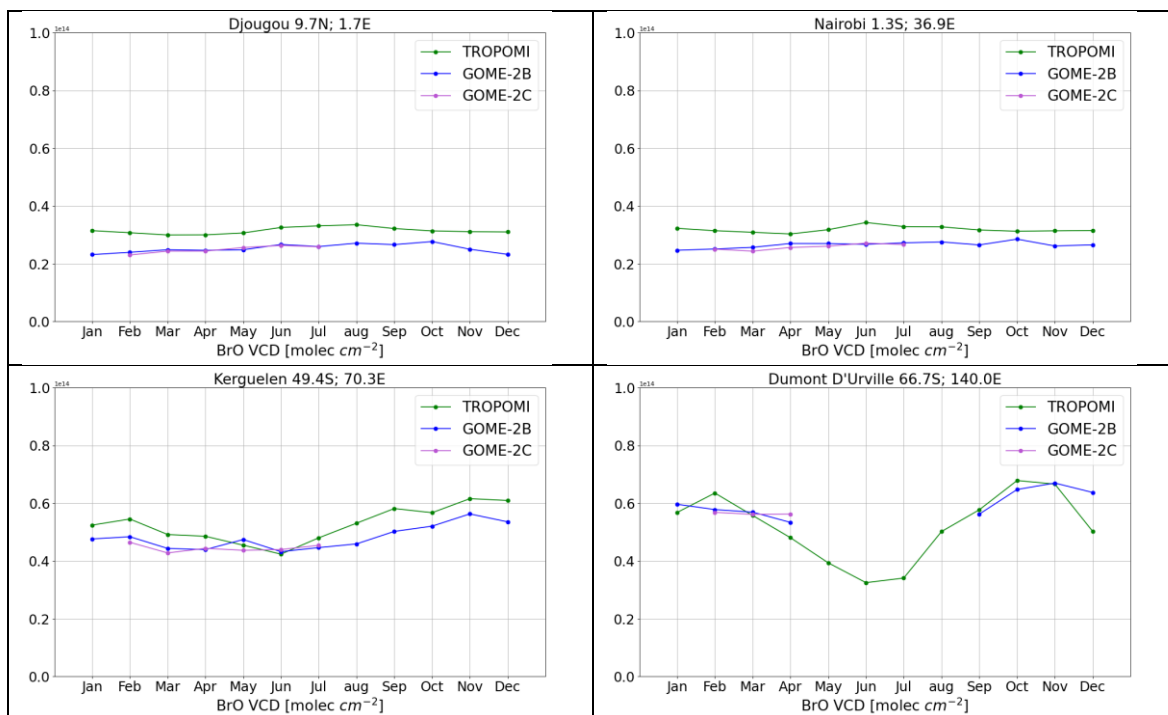


Figure continues on next page.



**Figure 9:** Comparison of TCBRO, GOME-2B, and GOME-2C BrO vertical column data over 12 ground stations.

### 6.3 TCBRO versus ground based data

TCBRO vertical BrO columns have been compared to zenith sky measurements from Harestua, Norway, for the year 2019. The ground-based columns are derived from vertical profiles retrieved by applying an Optimal Estimation-based profiling technique to zenith-sky measurements at sunrise (Hendrick et al., 2007). The sensitivity of these measurements to the troposphere is increased by using a fixed reference spectrum corresponding to clear-sky noon summer conditions for the spectral analysis. In order to ensure the photochemical matching between satellite and ground-based observations, the sunrise ground-based columns were photochemically converted to the satellite overpass solar zenith angles using a stacked box photochemical model (Hendrick et al., 2007 and 2008).

The comparison is shown in Figure 10. The TCBRO TROPOMI columns agree remarkably well with the zenith-sky columns for the time frame March-October 2019, with an offset of only  $-0.2 \pm 9\%$ . This confirms that at least part of the positive offset of the TROPOMI VCD's with respect to GOME-2 (B and C) values lies in the negative bias of the GOME-2 data with respect to the Harestua results (see Table 2).

TCBRO/TROPOMI	GOME-2B	GOME-2C
$-6 \pm 12 \%$	$-15 \pm 11\%$	$-12 \pm 10$
$-0.2 \pm 9\%$ (March-October)		

**Table 2:** Offset of the satellite BrO VCD data sets with respect to the Harestua zenith-sky measurements.

In the winter months, the TCBRO columns show a negative bias and this is likely related to the geometric approximation of the used AMF. Despite the high surface albedo in wintertime, the low sun implies a less accurate AMF and this effect should be further investigated by testing AMF values at different ground stations using local vertical BrO profiles. A similar effect was observed for the two GOME-2 instruments by Merlaud et al. (2020).

For a full understanding of the accuracy of the TCBRO columns, comparisons with more ground measurements at different locations would be useful.

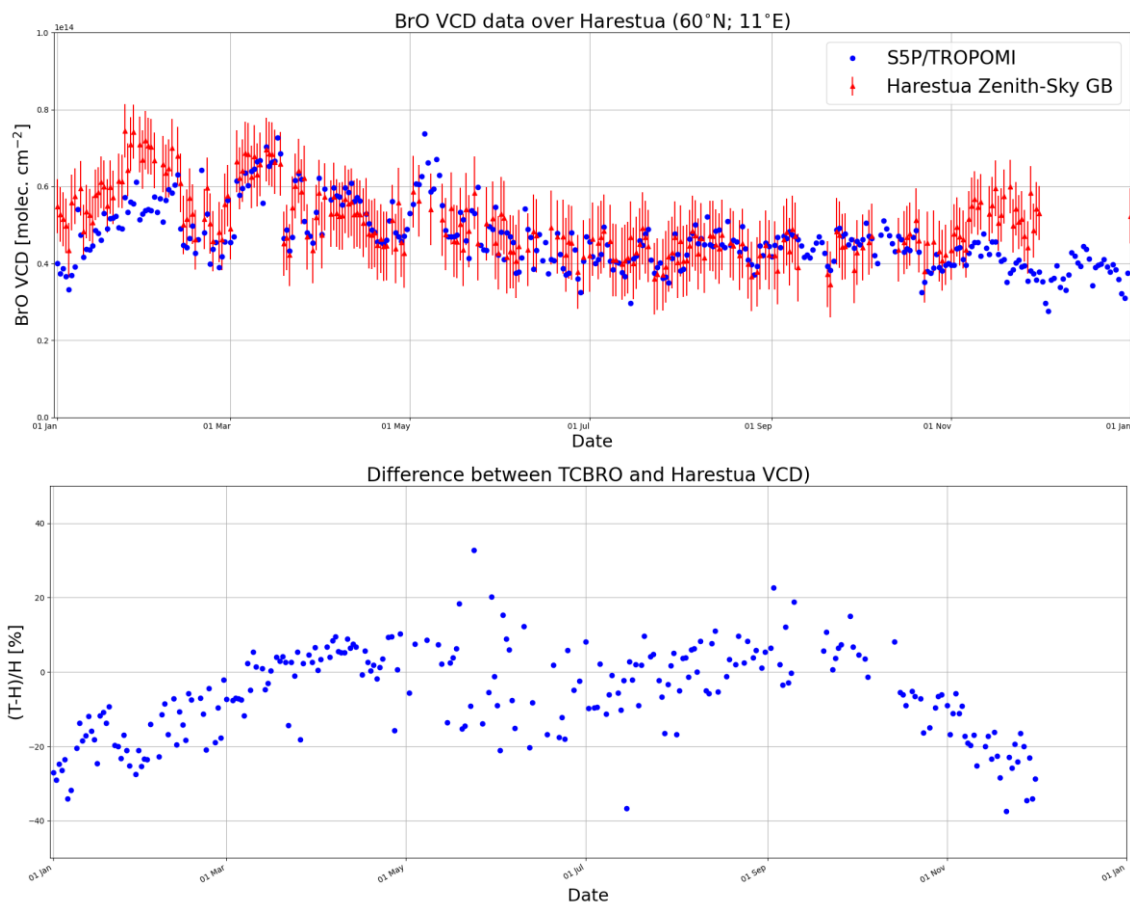


**Figure 10:** Daily BrO vertical column data as measured from Harestua (red) and with TROPOMI (blue). The two datasets agree well for the period March-October 2019.

## 7 Conclusions

This document described the first validation exercises of one year (2019) of data from the S5P total BrO algorithm TCBRO (version 1.1.1).

Both SCD and VCD data from TCBRO compare well with the reference satellite data, although TCBRO VCD's have a positive bias with respect to the two GOME-2 instruments. The agreement of TCBRO VCD data with Harestua zenith-sky measurement is very good ( $-0.2\pm 9\%$ ) and comparison with other (satellite and/or ground-based) data will be performed in the future to obtain more insight in the accuracy of the TCBRO columns.

## Appendix A – Monthly averaged BrO VCD for the full year 2019.

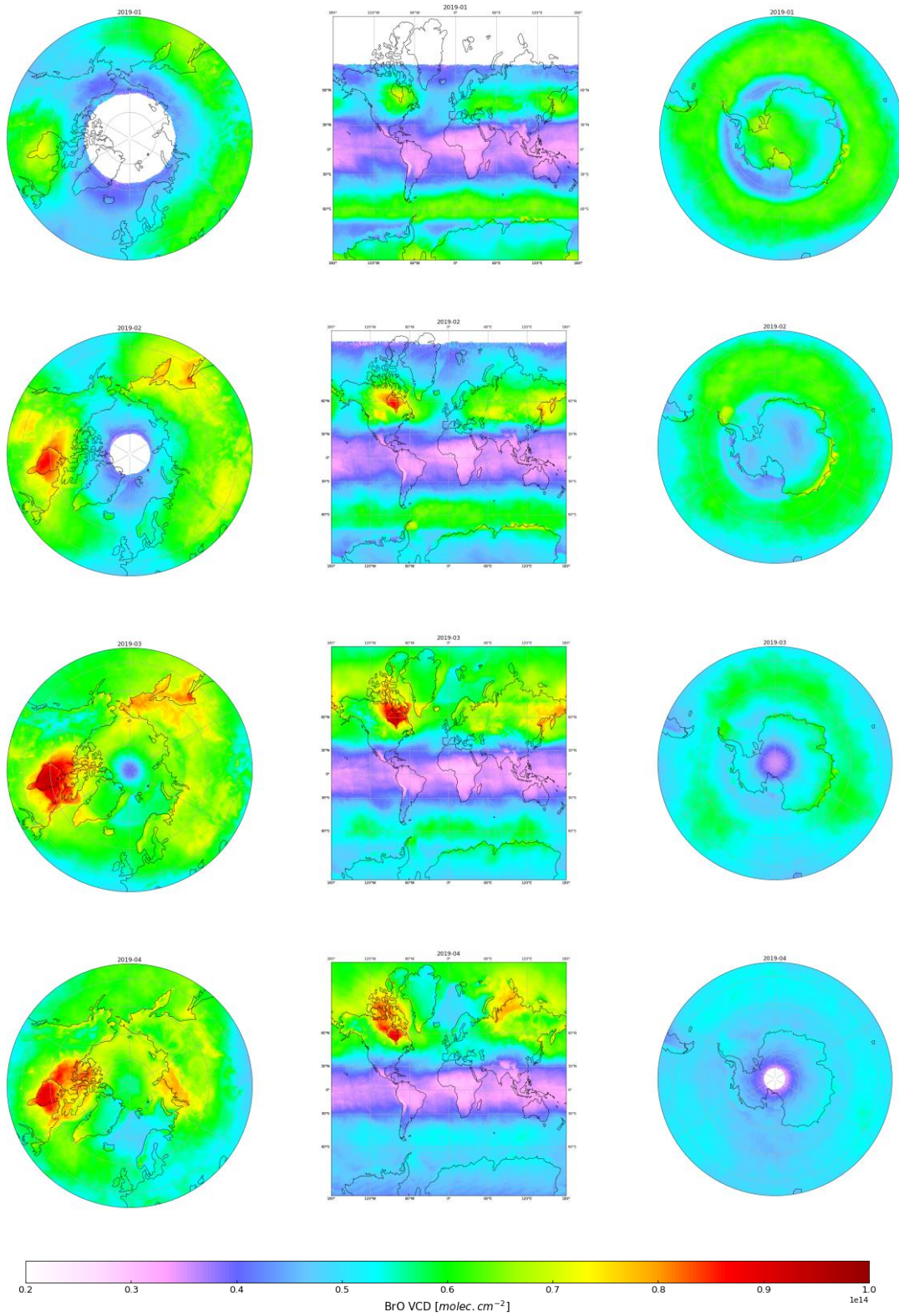


Figure continues on the next page.

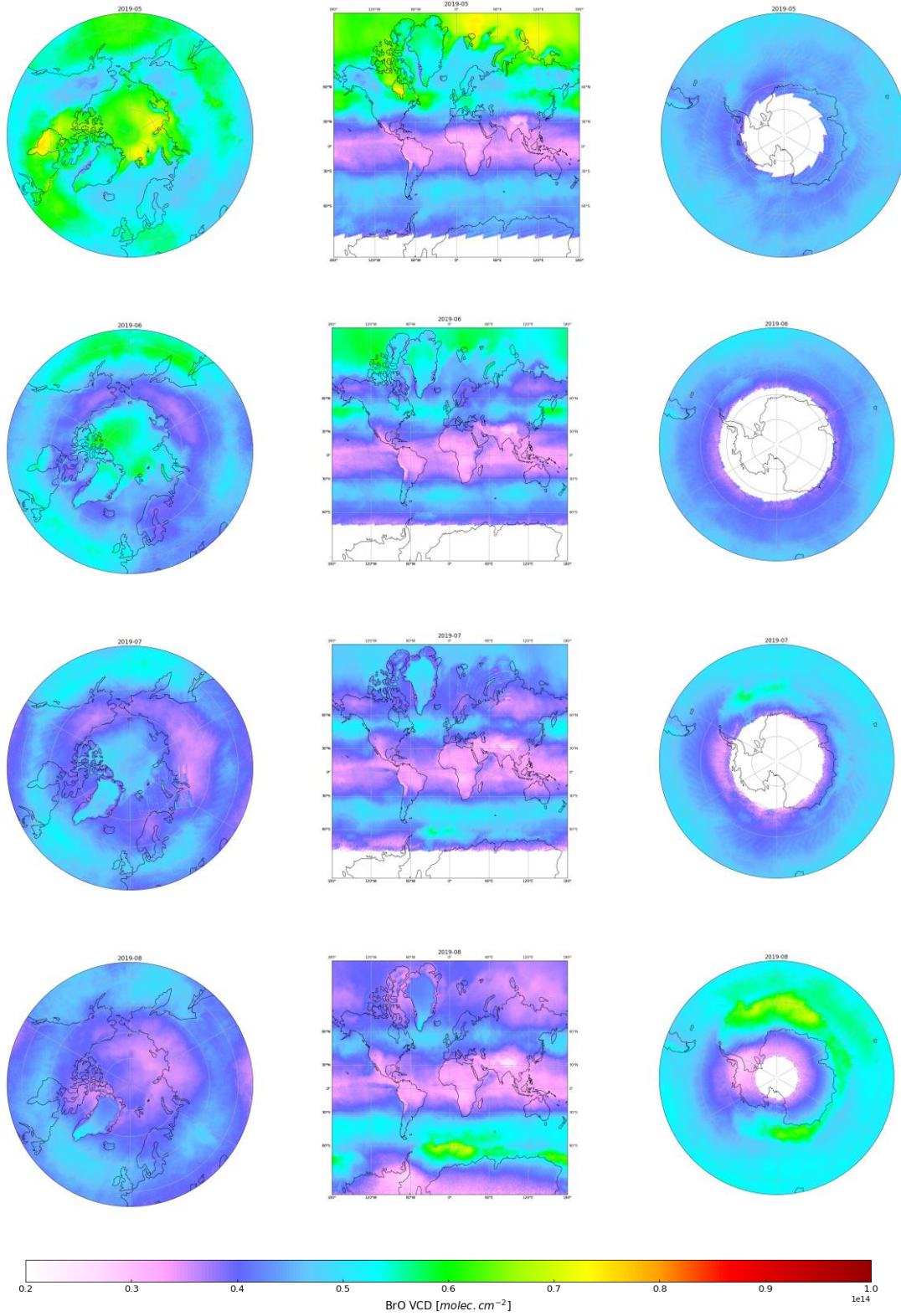
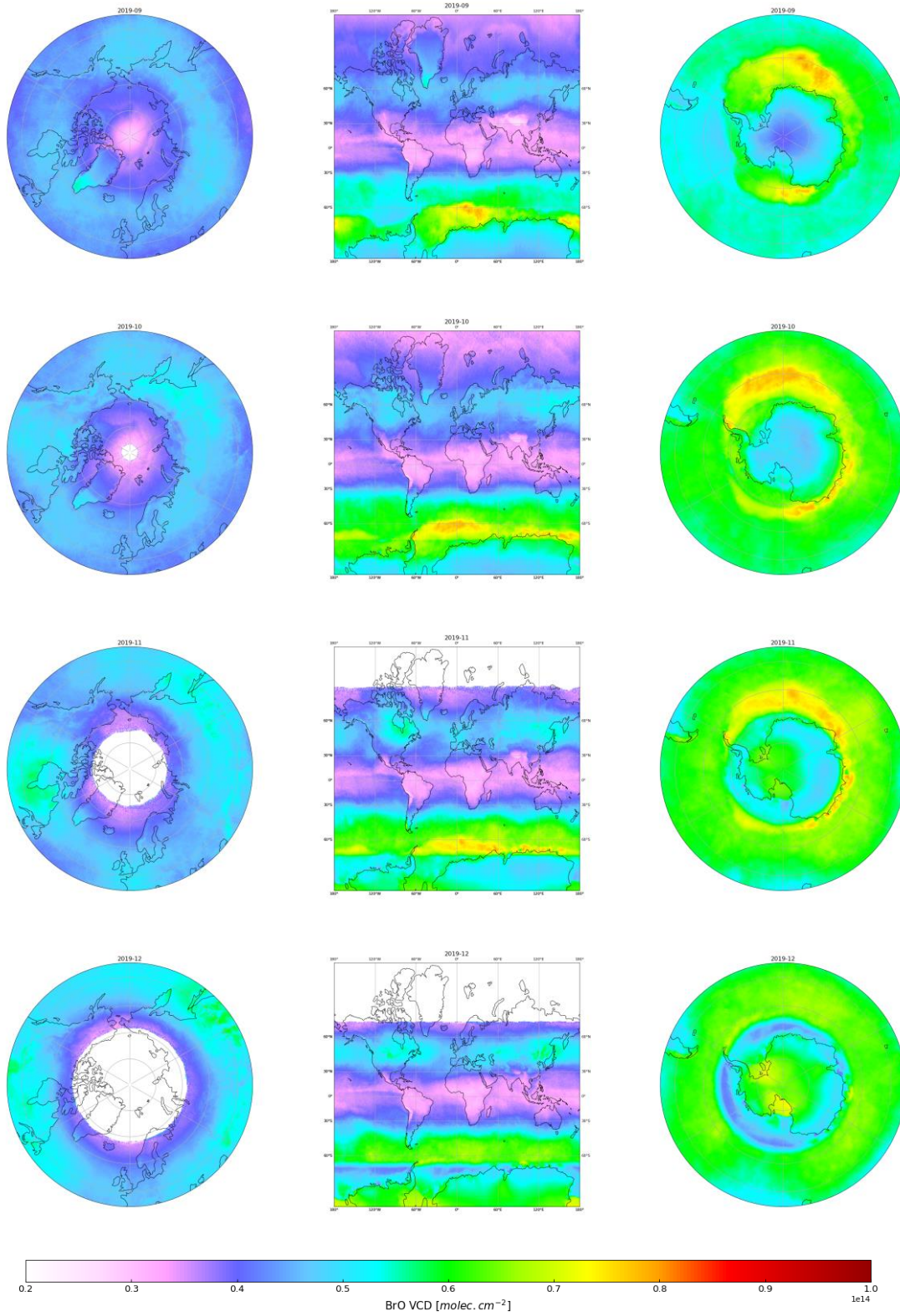


Figure continues on the next page.



**Figure 11:** S5P/TROPOMI monthly average BrO vertical column density (VCD) for the full year 2019. Left column: North Pole region; middle column: global distribution (Mercator); right column: South pole region.

## References

- Bogumil, K., Orphal, J., Homann, T., Voigt, S., Spietz, P., Fleischmann, O.C., Vogel, A., Hartmann, M., Bovensmann, H., Frerick, J., and Burrows, J.P., Measurements of molecular absorption spectra with the SCIAMACHY pre-flight model: Instrument characterization and reference data for atmospheric remote sensing in the 230-2380 nm region, *J. Photochem. Photobiol. A: Chem.* 157, 167-184 (2003); DOI: 10.1016/S1010-6030(03)00062-
- Bougoudis, I., Blechschmidt, A.-M., Richter, A., Seo, S., Burrows, J. P., Theys, N., and Rinke, A.: Long-term time series of Arctic tropospheric BrO derived from UV-VIS satellite remote sensing and its relation to first-year sea ice, *Atmos. Chem. Phys.*, 20, 11869–11892, <https://doi.org/10.5194/acp-20-11869-2020>, 2020.
- Chance, K. and R. J. Spurr: Ring effect studies: Rayleigh scattering including molecular parameters for rotational Raman scattering, and the Fraunhofer spectrum, *Applied Optics*, 36, 5224-5230, 1997.
- Chance, K. and Kurucz, R. L.: An improved high-resolution solar reference spectrum for earth's atmosphere measurements in the ultraviolet, visible, and near infrared, *J. Quant. Spectrosc. Radiat. Transf.*, 111(9), 1289-1295, 2010.
- Fayt, C. and M. Van Roozendaal: *Windoas 2.1, Software User Manual*, BIRA-IASB, 2001.
- Danckaert, T., Fayt, C., Van Roozendaal, M., De Smedt, I., Letocart, V., Merlaud, A., Pinardi, G: *Qdoas Software User Manual, Version 2.1*, [http://uv-vis.aeronomie.be/software/QDOAS/QDOAS\\_manual\\_2.1\\_201212.pdf](http://uv-vis.aeronomie.be/software/QDOAS/QDOAS_manual_2.1_201212.pdf), 2012.
- Fleischmann, O. C., et al. : New ultraviolet absorption cross-sections of BrO at atmospheric temperatures measured by time-windowing Fourier transform spectroscopy, *J. Photochem. Photobiol. A*, 168, 117–132, 2004.
- Hendrick, F., M. Van Roozendaal, M. P. Chipperfield, M. Dorf, F. Goutail, X. Yang, C. Fayt, C. Hermans, K. Pfeilsticker, J.-P. Pommereau, J. A. Pyle, N. Theys, and M. De Mazière, Retrieval of stratospheric and tropospheric BrO profiles and columns using ground-based zenith-sky DOAS observations at Harestua, 60°N, *Atmospheric Chemistry and Physics*, 7, 4869-4885, 2007
- Hendrick, F., Johnston, P.V., De Mazière, M., Fayt, C., Hermans, C., Kreher, K., Theys, N., and Van Roozendaal, M.: One-decade trend analysis of stratospheric BrO over Harestua (60°N) and Lauder (45°S) reveals a decline, *Geophys. Res. Lett.*, 35, L14801, doi:10.1029/2008GL034154, 2008.
- Hörmann, C., Sihler, H., Beirle, S., Penning de Vries, M., Platt, U., and Wagner, T.: Seasonal variation of tropospheric bromine monoxide over the Rann of Kutch salt marsh seen from space, *Atmos. Chem. Phys.*, 16, 13015–13034, <https://doi.org/10.5194/acp-16-13015-2016>, 2016.
- Meller, R., and Moortgat, G. K.: Temperature dependence of the absorption cross section of HCHO between 223 and 323K in the wavelength range 225–375 nm, *J. Geophys. Res.*, 105(D6), 7089–7102, doi:10.1029/1999JD901074, 2000.
- Merlaud, A., Theys, N., Hendrick, F., Van Gent, J., Pinardi, G., Van Roozendaal, M., Chan, K. L., Heue, K. P., and Valks, P.: Validation report of GOME-2 GDP 4.9 BrO column data for MetOp-C Operational Readiness Review, AC-SAF Validation Report, version 1.1, 19 May 2020, [https://acsaf.org/docs/vr/Validation\\_Report\\_OTO\\_BrO\\_May\\_2020.pdf](https://acsaf.org/docs/vr/Validation_Report_OTO_BrO_May_2020.pdf)
- Puķīte, J., Kühl, S., Deutschmann, T., Platt, U., and Wagner, T.: Extending differential optical absorption spectroscopy for limb measurements in the UV, *Atmos. Meas. Tech.*, 3, 631-653, 2010.
- Seo, S., Richter, A., Blechschmidt, A.-M., Bougoudis, I., and Burrows, J. P.: First high-resolution BrO column retrievals from TROPOMI, *Atmos. Meas. Tech.*, 12, 2913–2932, <https://doi.org/10.5194/amt-12-2913-2019>, 2019.
- Serdyuchenko, A., Gorshchev, V., Weber, M., Chehade, W., and Burrows, J. P.: High spectral resolution ozone absorption cross-sections – Part 2: Temperature dependence, *Atmos. Meas. Tech.*, 7, 625-636, doi:10.5194/amt-7-625-2014, 2014.
- Thalman, R. and Volkamer, R.: Temperature dependent absorption cross-sections of O2-O2 collision pairs between 340 and 630 nm and at atmospherically relevant pressure., *Phys. Chem. Chem. Phys.*, 15(37), 15371–81, doi:10.1039/c3cp50968k, 2013.
- Theys, N., Van Roozendaal, M., Errera, Q., Hendrick, F., Daerden, F., Chabrilat, S., Dorf, M., Pfeilsticker, K., Rozanov, A., Lotz, W., Burrows, J. P., Lambert, J.-C., Goutail, F., Roscoe, H. K., and De Mazière, M.: A global stratospheric bromine monoxide climatology based on the BASCOE chemical transport model, *Atmos. Chem. Phys.*, 9, 831-848, 2009.
- Theys, N., Van Roozendaal, M., Hendrick, F., Yang, X., De Smedt, I., Richter, A., Begoin, M., Errera, Q., Johnston, P. V., Kreher, K., and De Mazière, M.: Global observations of tropospheric BrO columns using GOME-2 satellite data, *Atmos. Chem. Phys.*, 11, 1791-1811, 2011.
- Theys, N., Hendrick, F., Van Gent, Van Roozendaal, M., Hao, N., and Valks, P.: Validation report of GOME-2 offline and reprocessed GDP 4.8BrO total column data for MetOp-A and B SAF/O3M/BIRA/VR/BRO/, O3M-SAF Validation Report, 9 Dec 2015, [https://acsaf.org/docs/vr/Validation\\_Report\\_OTO\\_DR\\_BrO\\_GDP48\\_Dec\\_2015.pdf](https://acsaf.org/docs/vr/Validation_Report_OTO_DR_BrO_GDP48_Dec_2015.pdf)

Vandaele A.C., C. Hermans, P.C. Simon, M. Carleer, R. Colin, S. Fally, M.F. Mérienne, A. Jenouvrier, and B. Coquart, Measurements of the NO<sub>2</sub> absorption cross-section from 42000 cm<sup>-1</sup> to 10000 cm<sup>-1</sup> (238-1000 nm) at 220 K and 294 K, J.Q.S.R.T., 59, 171-184, 1998.